

See discussions, stats, and author profiles for this publication at: <https://www.researchgate.net/publication/316652396>

Effect of surface crystallization on magnetic properties of Fe 82 Cu 1 Si 4 B 11.5 Nb 1.5 nanocrystalline alloy ribbons

Article in Journal of Magnetism and Magnetic Materials · May 2017

DOI: 10.1016/j.jmmm.2017.04.086

CITATIONS

0

READS

18

9 authors, including:



Fangpei Wan

Taiyuan University of Technology

4 PUBLICATIONS 2 CITATIONS

[SEE PROFILE](#)



Anding Wang

City University of Hong Kong

34 PUBLICATIONS 203 CITATIONS

[SEE PROFILE](#)



Chuntao Chang

Ningbo Institute of Materials Technology and...

101 PUBLICATIONS 1,495 CITATIONS

[SEE PROFILE](#)

Some of the authors of this publication are also working on these related projects:



Soft magnetic material [View project](#)



Research articles

Effect of surface crystallization on magnetic properties of Fe₈₂Cu₁Si₄B_{11.5}Nb_{1.5} nanocrystalline alloy ribbons



Jianhua Zhang ^{a,b,c,*}, Fangpei Wan ^{a,b,c}, Yecheng Li ^{a,b,c}, Jiecheng Zheng ^{a,b,c}, Anding Wang ^{d,e,*}, Jiancheng Song ^{a,b,c}, Muqin Tian ^{a,b,c}, Aina He ^{d,e,*}, Chuntao Chang ^{d,e}

^a Taiyuan University of Technology, No.79 Yingze West Avenue, Wanbolin District, Taiyuan, Shanxi 030024, China

^b College of Electrical and Power Engineering, Shanxi Key Laboratory of Coal Mining Equipment and Safety Control, Taiyuan University of Technology, No.79 Yingze West Avenue, Wanbolin District, Taiyuan, Shanxi 030024, China

^c National & Provincial Joint Engineering Laboratory of Mining Intelligent Electrical Apparatus Technology, Taiyuan University of Technology, No.79 Yingze West Avenue, Wanbolin District, Taiyuan, Shanxi 030024, China

^d Key Laboratory of Magnetic Materials and Devices, Ningbo Institute of Materials Technology and Engineering, Chinese Academy of Sciences, Ningbo, Zhejiang 315201, China

^e Zhejiang Province Key Laboratory of Magnetic Materials and Application Technology, Ningbo Institute of Materials Technology and Engineering, Chinese Academy of Sciences, Ningbo 315201, China

ARTICLE INFO

Article history:

Received 28 February 2017

Received in revised form 27 April 2017

Accepted 29 April 2017

Available online 2 May 2017

Keywords:

Nanocrystalline alloy

Soft magnetic property

Surface crystallization

Melt-spun

Pinning field

ABSTRACT

In this study, Fe₈₂Cu₁Si₄B_{11.5}Nb_{1.5} nanocrystalline alloy ribbons with completely amorphous structure and surface crystallization were prepared using melt-spinning technique with wheel speeds of 45 m/s, 35 m/s and 25 m/s. The effect of surface crystallization layers on the soft-magnetic properties, core loss and dynamic magnetization process were systematically investigated. Moreover, the permeability-frequency spectra were measured as a function of the AC magnetic field, ranging from 1 to 75 A/m. It was found that decreasing the melt-spinning wheel speed can widen the annealing temperature range and the coercivity increases with the increase of surface crystallization. Excessive crystallization layers will increase the pinning field (H_p), which will lead to an increase of magnetic anisotropy constant K and eventually decrease the effective permeability. The crystallization mechanism of the Fe₈₂Cu₁Si₄B_{11.5}Nb_{1.5} nanocrystalline alloy ribbons with surface crystallization layers was discussed from the aspects of diffusion and competitive processes, which is helpful for further understanding the nanocrystallization process.

© 2017 Elsevier B.V. All rights reserved.

1. Introduction

Recently, nanocrystalline soft magnetic alloys have attracted worldwide attention due to their excellent magnetic properties, including low core loss because of the low eddy currents in the high frequency range, high effective permeability (μ_e), low saturation magnetostriction (λ_s) and relatively high saturation magnetic flux density (B_s) [1,2]. Since the first development of Fe_{73.5}Si_{13.5}B₉Nb₃Cu₁ (Hitachi ®Finemet) in 1988 [3], a great many of efforts have been made to apply this nanocrystalline alloy in the electrical

equipment, such as transformers, common mode choke cores, inductors, motors and many other soft magnetic devices [4–6]. However, the B_s of the representative Fe_{73.5}Si_{13.5}B₉Nb₃Cu₁ alloy is only about 1.24 T because of the low Fe content and high Nb content. Developing nanocrystalline soft magnetic alloys with high B_s is extremely desired to realize the miniaturization and high efficiency of electrical equipment.

It is well known that B_s is directly related to the amount of magnetic transition metals (Fe, Co, Ni) and the crystallization volume fraction of α -Fe phase [7]. Since the crystallization volume fraction is relatively easy to control by the annealing process which is liable to realize, improving the Fe content may be the best way to enhance the B_s in FeSiBNbCu alloy system taking the raw materials cost into consideration. For these high B_s nanocrystalline alloys [8,9], the glass-forming-ability (GFA) is close to the upper limit of a single amorphous formation for conventional melt-spinning technology [10]. Therefore, the amorphous structure of Fe-rich nanocrystalline ribbons will be easily affected by many other

* Corresponding authors at: Taiyuan University of Technology, No.79 Yingze West Avenue, Wanbolin District, Taiyuan, Shanxi 030024, China (J. Zhang). Key Laboratory of Magnetic Materials and Devices, Ningbo Institute of Materials Technology and Engineering, Chinese Academy of Sciences, Ningbo, Zhejiang 315201, China (A. Wang). Zhejiang Province Key Laboratory of Magnetic Materials and Application Technology, Ningbo Institute of Materials Technology and Engineering, Chinese Academy of Sciences, Ningbo 315201, China (A. He).

E-mail addresses: zhangjianhua@tyut.edu.cn (J. Zhang), anding.w@hotmail.com (A. Wang), hean@nimte.ac.cn (A. He).

factors during the melt-spinning process, such as oxidation at the surface which will trigger crystallization, depletion of metalloids in the surface region, lower cooling rate [11]. As a result, partial crystallization will occur in the as-cast state, especially at the free side of the ribbons. Generally, it is well accepted that such a surface crystallization layer results in an out-of-plane magnetic anisotropy and, hence, affects the soft magnetic properties significantly [12,13]. However, for some situations, the completely amorphous state is not always advantageous, instead, partial crystallization may lead to improved or even novel properties [12]. In our study, we choose our newly developed $\text{Fe}_{82}\text{Cu}_1\text{Si}_4\text{B}_{11.5}\text{Nb}_{1.5}$ nanocrystalline alloy ribbons to study the effect of various surface crystallization degree on the soft-magnetic properties, domain walls, core loss and dynamic magnetization process. It was interestingly found that appropriate surface crystallization will improve the soft magnetic properties and reduce the core loss. Therefore, this study is benefits to have a better understanding of the effect of surface crystallization on the soft magnetic properties and microstructure evolution.

2. Experimental procedure

Multicomponent alloy ingot with nominal composition of $\text{Fe}_{82}\text{Cu}_1\text{Si}_4\text{B}_{11.5}\text{Nb}_{1.5}$ was prepared by induction melting the mixtures of pure Fe (99.99 wt%), Si (99.999 wt%), B (99.8 wt%), Nb (99.99 wt%), and Cu (99.99 wt%) under a high-purity argon atmosphere. The as-spun ribbons with good ductility were prepared using the single-roller melt-spinning method at the speeds of 45 m/s (S45), 35 m/s (S35) and 25 m/s (S25) in argon atmosphere. The thicknesses of ribbons were qualitatively determined by spiral micrometer. Thermodynamic properties of the as-spun alloys were evaluated by differential scanning calorimetry (DSC, NETZSCH 404C) at a heating rate of 0.67 °C/s under an argon flow. The as-spun ribbons were cut into 75 mm in length, then subjected to annealing in the absence of magnetic field at various temperatures for 10 min in a vacuum furnace and subsequently quenched in water with room temperature. The microstructures of the as-quenched and annealed ribbons were identified by X-ray diffraction (XRD, Bruker D8 Advance) with Cu-K α radiation. Average grain size of the nanocrystalline grains was estimated by using Scherrer equation from the full width at half maximum for the bcc (110) reflection peak. The permeability-frequency spectra of $\text{Fe}_{82}\text{Cu}_1\text{Si}_4\text{B}_{11.5}\text{Nb}_{1.5}$ annealed ribbons were measured with a vector impedance analyzer under different AC magnetic fields, ranging from 1 to 75 A/m. H_c were measured by using a DC B-H hysteresis loop tracer under a field of 1000 A/m. μ_e at 1 kHz was measured with a vector impedance analyzer under a field of 1 A/m. All measurements were carried out at room temperature.

3. Results and discussion

3.1. Ribbons with surface crystallization layers

The as-spun ribbons with thickness of 23–34 μm were prepared by single-roller melt-spinning method with different wheel speeds. The XRD patterns, shown in Fig. 1(a), were measured from the free side of the ribbons and only the XRD of S45 shows a broad intensity peak which indicates the ribbon is almost completely amorphous. With the decrease of wheel speed, the XRD patterns of S35 and S25 show sharp peaks at about 45° and 65° belonging to bcc α -Fe crystalline phase which can be confirmed in Fig. 7. The XRD patterns from the wheel side of all the samples show a fully amorphous structure, which means partial crystallization only appeared at the free side. Subsequently, the free surface layers with a thickness of 1 μm for S35 and S25 were removed by polish-

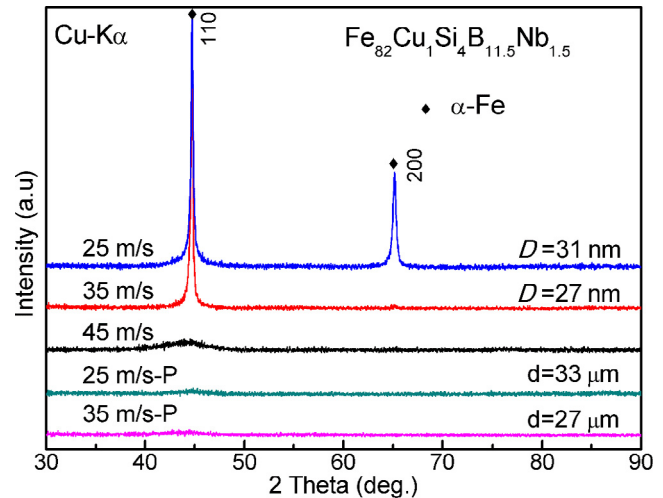


Fig. 1. XRD patterns of the melt-spun $\text{Fe}_{82}\text{Cu}_1\text{Si}_4\text{B}_{11.5}\text{Nb}_{1.5}$ ribbons with different wheel speeds and the S25 and S35 after removing a thickness of 1 μm at the free surface.

ing softly with metallographic abrasive paper. Then, as shown in the Fig. 1, amorphous structures for the two samples were obtained and the results indicate that the thickness of the surface crystallization layers is thinner than 1 μm .

The effect of surface crystallization layers on the thermodynamic properties of the melt-spun alloy ribbons were investigated by DSC at a heating rate of 0.67 K/s in a pure argon flow. As shown in Fig. 2, the onset temperature of the first crystallization process (T_{x1}) and the second crystallization process (T_{x2}) are almost keep the same values despite of the wheel speed. Since the area of the first exothermic peak is the exothermic values (ΔH) of the α -Fe precipitation, the crystallization volume fraction can be expressed as $V_{\text{cry}} = \Delta H_1 / \Delta H_2$, where ΔH_1 and ΔH_2 are the exothermic values of the samples with crystalline and the polished samples, respectively [14]. Therefore, the crystallization volume fraction of S35 and S25 can be obtained and the values are 3.1% and 3.3%, respectively.

3.2. Magnetic properties and core loss

In order to investigate the effect of surface crystallization layers on the soft magnetic properties of $\text{Fe}_{82}\text{Cu}_1\text{Nb}_{1.5}\text{Si}_4\text{B}_{11.5}$ ribbons, the

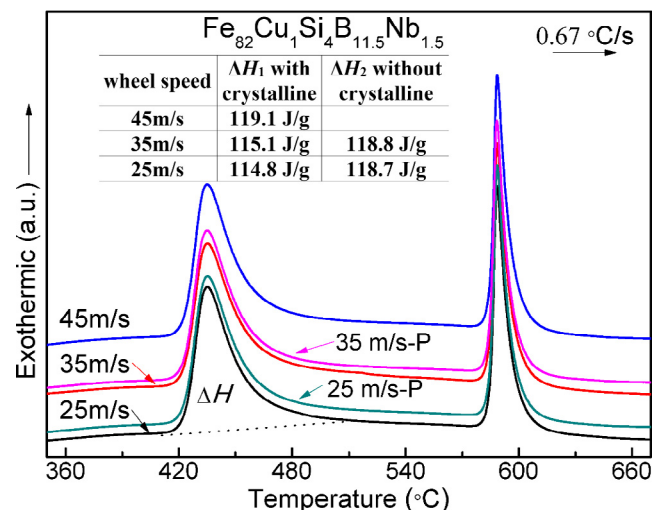


Fig. 2. DSC curves of the as-spun and the polished $\text{Fe}_{82}\text{Cu}_1\text{Nb}_{1.5}\text{Si}_4\text{B}_{11.5}$ ribbons with different wheel speeds.

changes of H_c and μ_e as a function of annealing temperature (T_A) for 10 min were measured. As shown in Fig. 3(a), with the increasing of the T_A , the H_c increases at first, and then rapidly decreases for all ribbons until 500 °C. S45 shows a minimum value of 8.9 A/m at 500 °C. S35 and S25 continue to decrease until 520 °C and reach minimum values of 9.5 A/m and 12.4 A/m, respectively. After reaching a minimum H_c , all samples show an increasing tendency with the T_A further increases. This trend of H_c can be understood based on the crystallization of the as-spun $\text{Fe}_{82}\text{Cu}_1\text{Nb}_{1.5}\text{Si}_4\text{B}_{11.5}$ alloy ribbons. The improvement of the soft-magnetic properties of the samples annealed between T_{x1} and T_{x2} is attributed to the precipitation of α -Fe with fine grain size and high density. While annealed at T_A higher than T_{x2} , the precipitation of the second phase will greatly degrade the soft-magnetic properties. In addition, it was found that the samples with surface crystallization layers show a wider annealing temperature range and the H_c increases with the higher degree of surface crystallization. The μ_e of all the alloys have a similar tendency in contrast to that of the H_c and the results were shown in Fig. 3(b). With the increase of T_A , μ_e decreases at first and then increases, followed by another decrease. The μ_e for S45, S35 and S25 annealed at the optimized annealing temperatures are 10,100, 12,700 and 9,200, respectively. It is interesting that the μ_e of S35 is much higher than other samples.

Since it is important to measure the core loss under various magnetic flux density (B) before applying any soft magnetic materials, the effect of surface crystallization on the core loss of the annealed $\text{Fe}_{82}\text{Cu}_1\text{Nb}_{1.5}\text{Si}_4\text{B}_{11.5}$ ribbons as a function of B were measured. As shown in Fig. 4, the core loss for all samples increase with the increases of B . It should be noticed that the sample with completely amorphous structure show much higher core loss than the samples with surface crystallization layers. With the decrease of wheel speed, the core loss exhibits a higher value than S35, but still lower than S45. The core loss at 1.0 T and 50 Hz ($P_{10/50}$) of S45, S35 and S25 are 0.27 W/kg, 0.20 W/kg and 0.23 W/kg, respectively. The core loss includes hysteresis loss which is relate to the area of the hysteresis loop and eddy current loss which is mainly dependent on the permeability for the similar size ribbons under the same conditions [15]. Since the B_s is similar about 1.67–1.70 T and the H_c exhibit increasing tendency with the decreases of wheel speed,

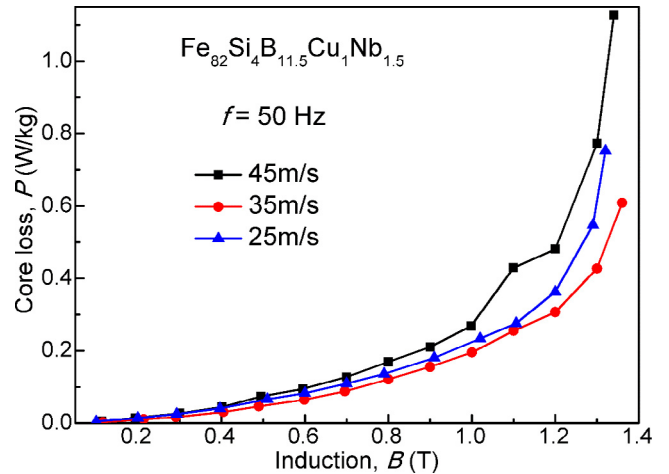


Fig. 4. The core loss dependent on the induction at 50 Hz of the $\text{Fe}_{82}\text{Cu}_1\text{Si}_4\text{B}_{11.5}\text{Nb}_{1.5}$ ribbons with different wheel speeds after annealing at optimal T_A for 10 min.

the samples with lower wheel speed should have a higher hysteresis loss. Therefore the lower core loss of S35 should be due to the high permeability.

3.3. Dynamic magnetization process and domains

Fig. 4 shows the permeability spectra of $\text{Fe}_{82}\text{Cu}_1\text{Si}_4\text{B}_{11.5}\text{Nb}_{1.5}$ ribbons annealed at optimal annealing condition measured under various applied AC field amplitudes. It is well known that there is a pinning field H_p in magnetic materials. When the applied field H is lower than H_p , the domain walls are pinned at the original sites and only reversible bowing of domain walls will occur, which is responsible for the initial increase of the permeability. For the higher field $H > H_p$, the domain walls are unpinned and irreversibly move to new positions, leading to hysteresis. When the exciting field increases from less than H_p to higher than H_p , we may observe a significant change of permeability occurs from frequency independent to frequency dependent. If H continues to increase, the domain wall motion corresponding to the knee part of magnetization curve may take place, then μ decreases [16].

As shown in Fig. 5(a), S35 has the highest μ_e and S25 exhibits the lowest μ_e . The permeability spectra were measured under more detail applied AC field amplitudes, but here just shown a few. It was shown that μ is almost constant and independent of the frequency in the low frequency region under a low applied AC field amplitude. μ increases with the increase of the applied AC field H , then decreases as H keeps increasing to a certain amplitude. All the curves merge into one line gradually in the high frequency region. According to classical magnetism, if $H > H_p$, the domain wall can move more easily in the material, then leads to a rise of μ ; if H goes on rising, domain wall motion corresponds to the knee part of magnetization curve, then decrease in μ occurs [16,17]. The H_p of S45, S35 and S25 are about 45 A/m, 45 A/m and 55 A/m, respectively. This indicates that the H_p will not considerably increase with the proper surface crystallization, while the excessive surface crystallization will lead to a drastic increase of magnetic anisotropy constant K [18,19], and as a result the permeability will decreases according to the Herzer's random anisotropy model [20].

Generally, the formation of surface crystallization layers will induce a compressive stress [13] and these stress plays an important role in the configuration of the domain structure and magnetic properties [21]. For further understanding the effect of different surface crystallization degree on the soft-magnetic properties,

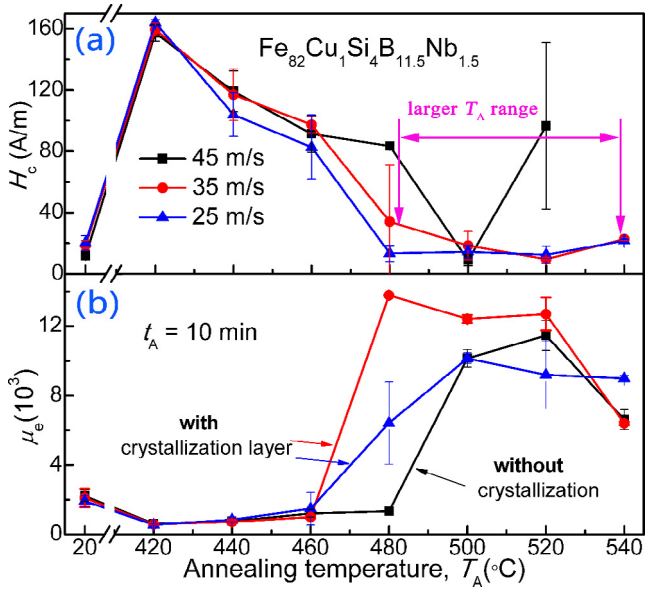


Fig. 3. T_A dependence of (a) H_c and (b) μ_e of $\text{Fe}_{82}\text{Cu}_1\text{Si}_4\text{B}_{11.5}\text{Nb}_{1.5}$ ribbons with different wheel speeds.

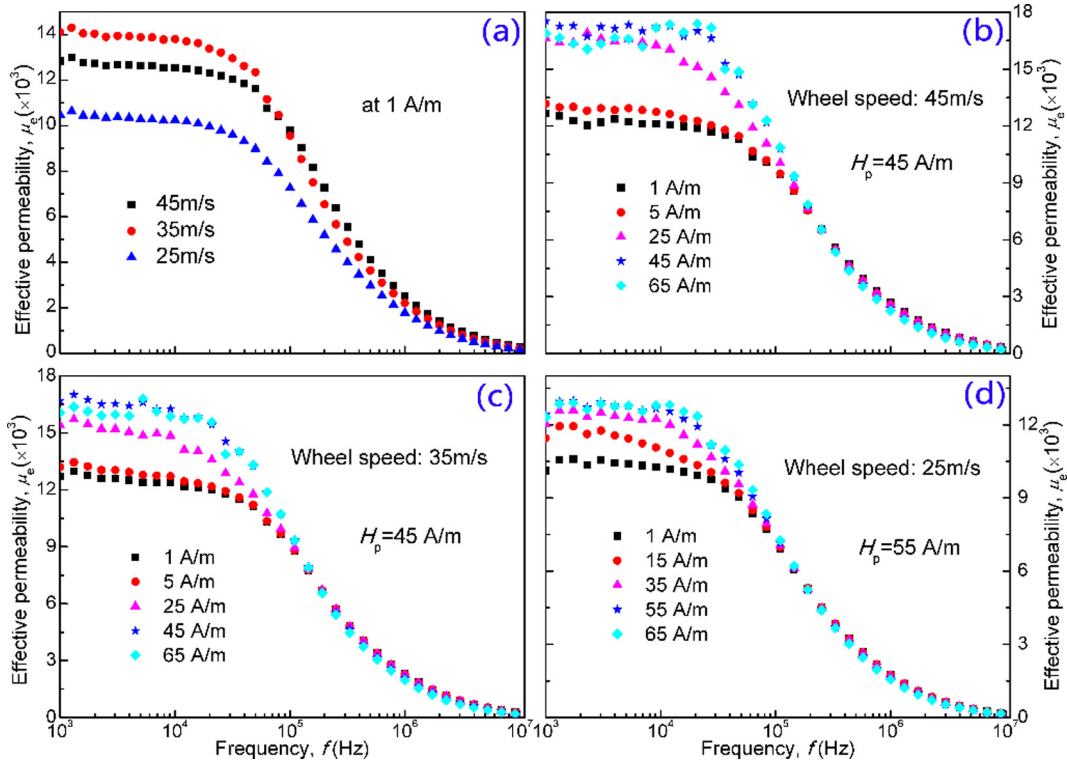


Fig. 5. Permeability spectra with various applied AC field amplitudes of $\text{Fe}_{82}\text{Cu}_1\text{Si}_4\text{B}_{11.5}\text{Nb}_{1.5}$ ribbons with different wheel speeds after annealing at optimal T_A for 10 min.

magnetic domains with clear border were examined under zero field with Magneto-optical Kerr Microscopy. It can be seen from Fig. 6 that for the as-spun $\text{Fe}_{82}\text{Cu}_1\text{Si}_4\text{B}_{11.5}\text{Nb}_{1.5}$ alloy ribbons with different wheel speeds, the domain magnetization direction (shown in Fig. 6(a and c)) is in transversal direction according to the previous study the quenched-in transversal stress will induce 180° domains [22]. According to the studies of Tejedor et al., the compressive stress will gradually change to tensile stress in the central part and the strong stress is the origin of transversal in-plane magnetic anisotropy [22]. After annealing, the angle between ribbon and domain directions changes from perpendicular to a certain value which means the in-plane magnetic anisotropy decreases dramatically after the residual stresses were removed [21,23]. In addition, the widths of the domain for S45 is larger than S35. It has been pointed that the widths of the domain is inversely proportional to the magnetic anisotropy [24] and the magnetic anisotropy will increase with the higher thickness of surface

crystallization layer [23,25]. This may be the main reason for the refining domain structures. While the Fig. 6(e and f) show nothing due to the rough surface of S25.

3.4. Microstructure evolution

In order to eliminate the influence of the grain size (D) of the surface crystalline on the average D , the ribbons were ground into powder before XRD measurement. As shown in Fig. 7, the average D which were calculated from (110) peak of the corresponding XRD pattern using Scherrer's equation show an abnormal decrease with the decrease of wheel speed, and the average D of S45, S35 and S25 are 19 nm, 18 nm and 15 nm, respectively.

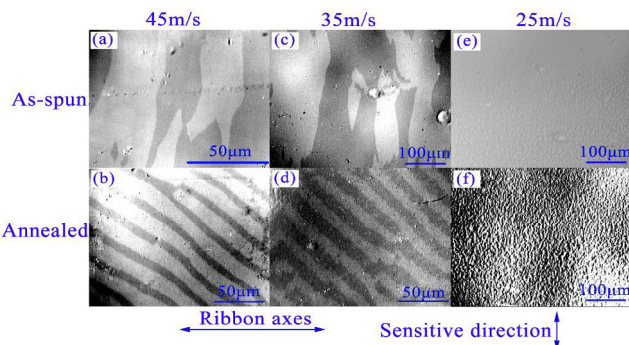


Fig. 6. Magnetic domain structure of as-spun and annealed $\text{Fe}_{82}\text{Cu}_1\text{Si}_4\text{B}_{11.5}\text{Nb}_{1.5}$ ribbons with different wheel speeds.

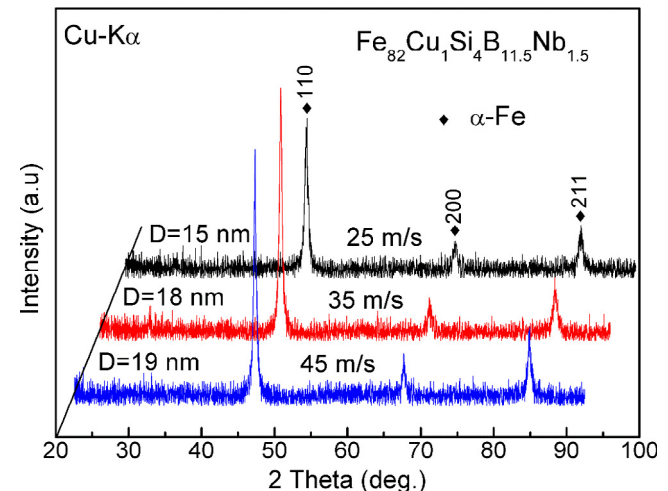


Fig. 7. XRD patterns of $\text{Fe}_{82}\text{Cu}_1\text{Si}_4\text{B}_{11.5}\text{Nb}_{1.5}$ alloys ribbons annealed at respective optimal annealing condition.

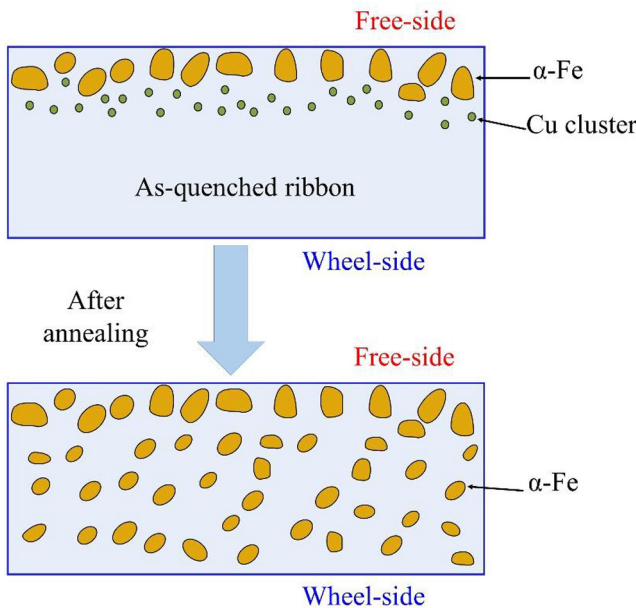


Fig. 8. Schematic diagram of the crystallization process of $\text{Fe}_{82}\text{Cu}_1\text{Si}_4\text{B}_{11.5}\text{Nb}_{1.5}$ alloys ribbons.

As with other FeSiBNbCu system alloys [2,3,26], the formation of nanocrystalline structure in our alloys also be ascribed to the mutual effect of Cu and Nb elements in the bcc Fe–Si [14,27]: Cu enhances the nucleation of the bcc α -Fe grains, while Nb impedes coarsening and inhibits the formation of other boride compounds. But the crystallization mechanism of $\text{Fe}_{82}\text{Cu}_1\text{Si}_4\text{B}_{11.5}\text{Nb}_{1.5}$ alloys with surface crystallization layers is slightly different and the schematic of the crystallization process was shown in Fig. 8. We suppose that the formation of nanocrystalline structure in $\text{Fe}_{82}\text{Cu}_1\text{Si}_4\text{B}_{11.5}\text{Nb}_{1.5}$ alloys may be driven by the combination of diffusion [28] and competitive process [29]. Since the nucleation of α -Fe is strongly relate to the amount of Cu clusters in FeSiBNbCu system alloys and the primary crystalline always exists in the as-quenched ribbons with low cooling rate, the as-quenched ribbons with surface crystallization layers should contain a great many of Cu clusters under the crystallization layers which serve as nuclei for heterogeneous nucleation of α -Fe crystallites during the annealing process. When annealing at the optimal condition, a large amount of α -Fe grains appeared in the ribbons because of the plenty of Cu clusters. The α -Fe nanocrystallites competitively grow up. At the same time, the Nb atoms were rejected from α -Fe nanocrystals and gathered around the grains. The diffusion of Fe via Nb-rich region (i.e. remaining amorphous matrix) is difficult and such area can act as an obstacle against Fe diffusion because of the large atomic radius of Nb. Hence, the fast growth of nanocrystal was suppressed both by the diffusion and competitive process. The grains need higher annealing temperature with the same annealing time to grow up which will result in large annealing temperature range and a smaller grain size than the completely amorphous ribbons. The results calculated from XRD patterns shown in Fig. 7 are also verified this nanocrystallization mechanism.

4. Conclusion

In summary, it was found that decreasing the melt-spinning wheel speed can widen the annealing temperature range for $\text{Fe}_{82}\text{Cu}_1\text{Si}_4\text{B}_{11.5}\text{Nb}_{1.5}$ ribbon and all samples show excellent soft-magnetic properties after annealing at optimal annealing conditions. Moreover, proper surface crystallization will decrease the core loss

from 0.27 W/kg to 0.20 W/kg without increasing the pinning field, but excessive surface crystallization will increase the pinning field, which may lead to a drastic increase of magnetic anisotropy constant K and eventually decrease the μ_e . The crystallization processes of the $\text{Fe}_{82}\text{Cu}_1\text{Si}_4\text{B}_{11.5}\text{Nb}_{1.5}$ nanocrystalline alloy ribbons with surface crystallization layers were driven by diffusion and competitive processes.

Acknowledgements

This work was supported by the National Natural Science Foundation of China (Grant Nos. 51541106, U1510112 and 51577123), Ningbo International Cooperation Projects (Grant No. 2015D10022), the National Key Research and Development Program of China (Grant No. 2016YFB0300501) and the Qualified Personnel Foundation of Taiyuan University of Technology (QPTF) (No: tyutrc-201370a).

References

- [1] M.A. Williard, Michael E. McHenry, David E. Laughlin, Amorphous and nanocrystalline materials for applications as soft magnets, *Prog. Mater. Sci.* 44 (1999) 291–433.
- [2] G. Herzer, Chapter3-nanocrystalline soft magnetic alloys, *Handbook Magn. Mater.*, 10, 1997, pp. 415–462.
- [3] Y. Yoshizawa, S. Oguma, K. Yamauchi, New Fe-based soft magnetic alloys composed of ultrafine grain structure, *J. Appl. Phys.* 64 (1988) 6044.
- [4] Y. Yoshizawa, K. Yamauchi, T. Yamane, H. Sugihara, Common mode choke cores using the new Fe-based alloys composed of ultrafine grain structure, *J. Appl. Phys.* 64 (1988) 6047.
- [5] K. Takenaka, N. Nishiyama, A.D. Setyawati, P. Sharma, A. Makino, Performance of a prototype power transformer constructed by nanocrystalline Fe-Co-Si-B-P-Cu soft magnetic alloys, *J. Appl. Phys.* 117 (2015).
- [6] N. Nishiyama, K. Tanimoto, A. Makino, Outstanding efficiency in energy conversion for electric motors constructed by nanocrystalline soft magnetic alloy "NANOMET (R)" cores, *Aip Adv.* 6 (2016) 055925.
- [7] M. Ohta, Y. Yoshizawa, Cu addition effect on soft magnetic properties in Fe–Si–B alloy system, *J. Appl. Phys.* 103 (2008) 07E722.
- [8] M. Ohta, Y. Yoshizawa, High Bs nanocrystalline $\text{Fe}_{84-x-y}\text{Cu}_x\text{Nb}_y\text{Si}_4\text{B}_{12}$ alloys ($x = 0.0–1.4$, $y = 0.0–2.5$), *J. Magn. Magn. Mater.* 321 (2009) 2220–2224.
- [9] F. Hosseini-Nasb, A. Beittollahi, M.K. Moravvej-Farshi, Effect of crystallization on soft magnetic properties of nanocrystalline $\text{Fe}_{80}\text{B}_{10}\text{Si}_4\text{Nb}_1\text{Cu}_1$ alloy, *J. Magn. Magn. Mater.* 373 (2015) 255–258.
- [10] A.D. Wang, H. Men, C.L. Zhao, C.T. Chang, R.W. Li, X.M. Wang, Crystallization behavior of FeSiBPc nanocrystalline soft-magnetic alloys with high fe content, *Sci. Adv. Mater.* 7 (2015) 2721–2725.
- [11] E. Lopatina, I. Soldatov, V. Budinsky, M. Marsilius, L. Schultz, G. Herzer, R. Schäfer, Surface crystallization and magnetic properties of $\text{Fe}_{84.3}\text{Cu}_{0.7}\text{Si}_4\text{B}_8\text{P}_3$ soft magnetic ribbons, *Acta Mater.* 96 (2015) 10–17.
- [12] G. Herzer, H.R. Hilzinger, Surface crystallisation and magnetic properties in amorphous iron rich alloys, *J. Magn. Magn. Mater.* 62 (1986) 143–151.
- [13] H.N. Ok, A.H. Morrish, Origin of the perpendicular anisotropy in amorphous $\text{Fe}_{82}\text{B}_{12}\text{Si}_6$ ribbons, *Phys. Rev. B* 23 (1981) 2257–2261.
- [14] F.P. Wan, T. Liu, F. Kong, A. Wang, M. Tian, J. Song, J. Zhang, C. Chang, X. Wang, Surface crystallization and magnetic properties of FeCuSiBNbMo melt-spun nanocrystalline alloys, *Mater. Res. Bull.* (2017), <http://dx.doi.org/10.1016/j.materresbull.2017.01.026>.
- [15] Y. Zhang, P. Pillay, M. Ibrahim, M.C. Cheng, Magnetic characteristics and core losses in machine laminations: high-frequency loss prediction from low-frequency measurements, *IEEE Trans. Ind. Appl.* 48 (2012) 623–629.
- [16] Y. Ding, T. Qiu, X. Liu, Y. Long, Y. Chang, R. Ye, Permeability-frequency spectra of $(\text{Fe}_{1-x}\text{Co}_x)_{73.5}\text{Cu}_1\text{Nb}_3\text{Si}_{13.5}\text{B}_8$ nanocrystalline alloys under different magnetic fields, *J. Magn. Magn. Mater.* 305 (2006) 332–335.
- [17] H. Liu, C. Yin, X. Miao, Z. Han, D. Wang, Y. Du, Permeability spectra study of $\text{Fe}_{73.5}\text{Si}_{13.5}\text{B}_9\text{Cu}_1\text{Nb}_{3-x}\text{Al}_x$ ($x = 0, 0.1, 0.2, 0.4, 0.8$ and 1.6), *J. Alloys Compd.* 466 (2008) 246–249.
- [18] Y. Yoshizawa, S. Fujii, D.H. Ping, M. Ohnuma, K. Hono, Magnetic properties of nanocrystalline Fe–Co–Cu–M–Si–B alloys (M: Nb, Zr), *Mater. Sci. Eng. A* 375–377 (2004) 207–212.
- [19] D.H.P.M. Ohnuma, T. Abe, H. Onodera, K. Hono, Y. Yoshizawa, Optimization of the microstructure and properties of co-substitute Fe–Si–B–Nb–Cu nanocrystalline soft magnetic alloys, *J. Appl. Phys.* 93 (2003) 9186–9194.
- [20] G. Herzer, Grain size dependence of coercivity and permeability in nanocrystalline ferromagnets, *IEEE Trans. Magn.* 26 (1990) 1397–1402.
- [21] C. Zhao, A. Wang, A. He, S. Yue, C. Chang, X. Wang, R.-W. Li, Correlation between soft-magnetic properties and $T_{x1}-T_c$ in high Bs FeCoSiBPC amorphous alloys, *J. Alloys Compd.* 659 (2016) 193–197.
- [22] M. Tejedor, J.A. Garcia, J. Carrizo, L. Elbaile, Mechanical determination of internal stresses in as-quenched magnetic amorphous metallic ribbons, *J. Mater. Sci.* 32 (1997) 2337–2340.

- [23] S. Flohrer, R. Schäfer, C. Polak, G. Herzer, Interplay of uniform and random anisotropy in nanocrystalline soft magnetic alloys, *Acta Mater.* 53 (2005) 2937–2942.
- [24] H. Krommüller, M. Fähnle, M. Domann, H. Grimm, R. Grimm, B. Gröger, Magnetic properties of amorphous ferromagnetic alloys, *J. Magn. Magn. Mater.* 13 (1979) 53–70.
- [25] Rudolf Schafer, N. Mattern, G. Herzer, Stripe domains on amorphous ribbons, *IEEE Trans. Magn.* 32 (1996) 4809–4811.
- [26] Q. Liu, J. Mo, H. Liu, L. Xue, L. Hou, W. Yang, L. Dou, B. Shen, L. Dou, Effects of Cu substitution for Nb on magnetic properties of Fe-based bulk metallic glasses, *J. Non-Cryst. Solids* 443 (2016) 108–111.
- [27] F.P. Wan, A. He, J. Zhang, J. Song, A. Wang, C. Chang, X. Wang, Development of FeSiBNbCu nanocrystalline soft magnetic alloys with high B_s and good manufacturability, *J. Electron. Mater.* 45 (2016) 4913–4918.
- [28] K. Hono, K. Hiraga, Q. Wang, A. Inoue, T. Sakurai, The microstructure evolution of a $\text{Fe}_{73.5}\text{Si}_{13.5}\text{B}_9\text{Nb}_3\text{Cu}_1$ nanocrystalline soft magnetic material, *Acta Metall. Mater.* 40 (1992).
- [29] P. Sharma, X. Zhang, Y. Zhang, A. Makino, Competition driven nanocrystallization in high B_s and low coreloss Fe–Si–B–P–Cu soft magnetic alloys, *Scr. Mater.* 95 (2015) 3–6.